Hendrik Meyer for the STEP Plasma, Control,
Heating & Current Drive Team, Contributors

The Physics of the Preferred Plasma Scenario for STEP

The Physics of the Preferred Plasma Scenario for STEP

Hendrik Meyer for the STEP Plasma, Control, Heating & Current
Drive Team, Contributors

The Physics of the Preferred Plasma Scenario for STEP

H Meyer[1] for the STEP Plasma, Control and Heating & Current Drive Team and Contributors
[1] United Kingdom Atomic Energy Authority, Culham Science Centre, Abingdon, Oxon, OX14 3DB, UK
e-mail (speaker): Hendrik.Meyer@ukaea.org.uk

Introduction: With steady progress on the ITER project and the design of DEMO, the international community is now entering an era in which fusion power on the grid could become a reality within the next $20 - 30$ years. In this environment the UK has started the ambitious Spherical Tokamak for Energy Production (STEP)[1] [2] programme, aiming to develop a compact prototype reactor based on the spherical tokamak (ST) concept by 2040 to deliver net electric power $P_{el} > 100$ MW to the grid. The programme has three tranches with the first providing a conceptual design of a STEP Prototype Plant (SPP) by Mar 2024. The ST concept makes it possible to maximise fusion power $P_{fus} \propto 1/A(\kappa\beta_N B_t)^4$ [3] and bootstrap current fraction $f_{BS} = I_{BS}/I_p$ in a compact device at relatively low toroidal field by allowing operation at high normalised pressure $\beta_N \approx 4 - 5$ and high elongation $\kappa > 2.8$, but it also poses unique challenges. The compactness restricts significantly the available inductive flux for the plasma pulse and therefore the required plasma current of $I_p \approx 20$ MA needs to be predominantly generated, maintained, and ramped-down non-inductively. In addition, it limits the space available for T breeding and plasma exhaust.

Plasma design tools: To design the plasma the integrated modelling suite JINTRAC, with the transport module JETTO at its core, has been adapted with suitable feedback mechanisms to model non-inductive plasmas with automatic current profile optimisation using genetic algorithms. A fast JETTO (f-JETTO) version has been developed for concept optimisation and sensitivity scanning using simplified models for heating and current drive (HCD), pellet fuelling and the pedestal performance. Here, f-JETTO is used as an assumption integrator using a Bohm-gyro-Bohm (BgB) model honed on JET and MAST to represent the dominant electron transport observed in an ST. This fast version uses outputs such as β_N, machine size and basic shape parameters from the systems code PROCESS, to derive a plasma solution for the flat-top operating point (FTOP) consistent with the transport assumptions and the sources and sinks. Using PROCESS and f-JETTO around 40 concept FTOPs have been produced to map the operational space. This included I-mode and negative triangularity concepts. In post-processing the global MHD stability, critical pedestal pressure as well as the vertical stability and α-particle confinement are assessed to give a valid operating point. The latter two require a free boundary equilibrium (FBE) calculated using FIESTA, a 2D first wall contour and a valid magnetic cage. Therefore, FBEs are calculated only for a selected number of concepts. Higher fidelity modules for the current drive, fuelling and transport are used to benchmark the assumptions of the reduced version. The DYON code – extended to only need coil currents and prefill conditions as input – is used to model the plasma initiation. MARS-F/K are used to develop RWM control as well as the suppression of edge localised modes (ELMs) using resonant magnetic perturbations. Using SOLPS-ITER (without drifts) feasible exhaust solutions are explored, and a reduced model for access to full detachment has been developed. A key activity is the validation of the BgB transport assumption using linear and non-linear gyrokinetic (GK) simulations. Codes like GRAY, GENRAY/CQL3D and ASCOT are used to model electron cyclotron HCD (ECCD), electron Bernstein wave HCD (EBW), ion cyclotron and Helicon wave heating and neutral beam HCD (NBCD) respectively. LOCUST is used to study the impact of 3D magnetic perturbations on the α-particle confinement, setting the requirements for the number and outer radius of the picture frame toroidal field coils.

Figure 1: Plasma current (top) and average confinement enhancement factor (bottom) as function of f_{GW} for constant P_{aux} and different fixed β_N values.

Basic plasma design principles: To enable both high κ and β_N simultaneously, a broad current profile with a low $l_i(3) \sim 0.25$ is needed. This favours operation above the no-wall limit, likely requiring active resistive wall mode (RWM) stabilisation. Access to 2nd stability as well as avoidance of low m/n neoclassical tearing modes (NTMs) favour a monotonic safety factor profile with $q_{min} > 2$. These requirements rule out a negative triangularity L-mode as calculations in such cases show a very low $\beta_N < 3$ (with $q_{min} \sim 1$) and $\kappa < 2$ stability limits. A substantial amount of the current density provided by the bootstrap current and auxiliary current
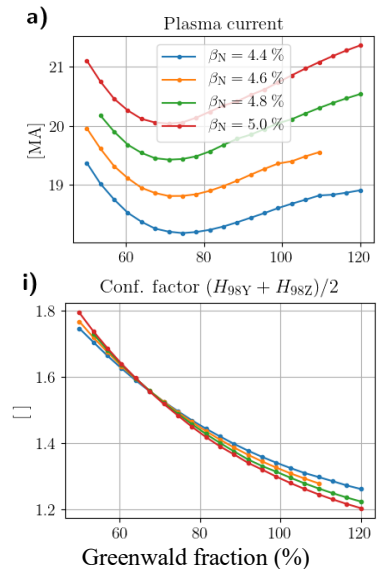
drive needs to be far off axis, whilst on-axis current drive is needed to avoid the formation of a current hole. To reduce the parasitic load the electrical power requirements for the auxiliary current drive need to be minimised in the burning flat-top phase whilst efficient auxiliary current drive is needed during the ramp-up (see below). Figure 1 shows the dependence of the plasma current (top) and the average confinement enhancement factor $\langle H_{98} \rangle = (H_{98} + H_{98}^{\star})/2$ for constant HCD power $P_{aux} = 150\ MW$ at different β_N values on the Greenwald fraction $f_{GW} = \langle n \rangle / n_{GW} = \pi a^2 \langle n \rangle / I_p$. Here, H_{98} is based on the ITER98 confinement scaling [4] taking the total radiated power into account, whilst $H_{98}^{\star}$ neglects the radiation. Both quantities are an output of the analysis which fixes β_N and P_{aux} varying the BgB transport assumption with a pre-factor. $\langle H_{98} \rangle$ is used on STEP because of the uncertainty of the radiation correction which depends on the electron heating profile and the radiation profile. In can be seen in Figure 1a that there is a minimum in I_p at $f_{GW} \sim 0.7$ caused by the decreasing auxiliary current drive efficiency and increasing I_{BS} due to increasing P_{fus} with density. The self-organising non-inductive scenario at high f_{BS} does not show the usual experimentally observed correlation $\beta_N \propto H_{98}$. To achieve the same β_N at lower f_{GW} with constant P_{aux} one needs to assume higher confinement. This favours operation at high $f_{GW} \sim 1$. To avoid the need for a difficult to integrate inboard blanket, an aspect ratio $A < 2$ needs to be chosen [5]. The possible inboard build then defines the minimum size of the device. Europed simulations of the pedestal performance scanning key parameters show a very strong increase of the achievable pedestal pressure with triangularity δ and a very small degradation with separatrix density favouring $\delta > 0.5$, though to achieve high triangularity coils relatively close to the plasma are needed.
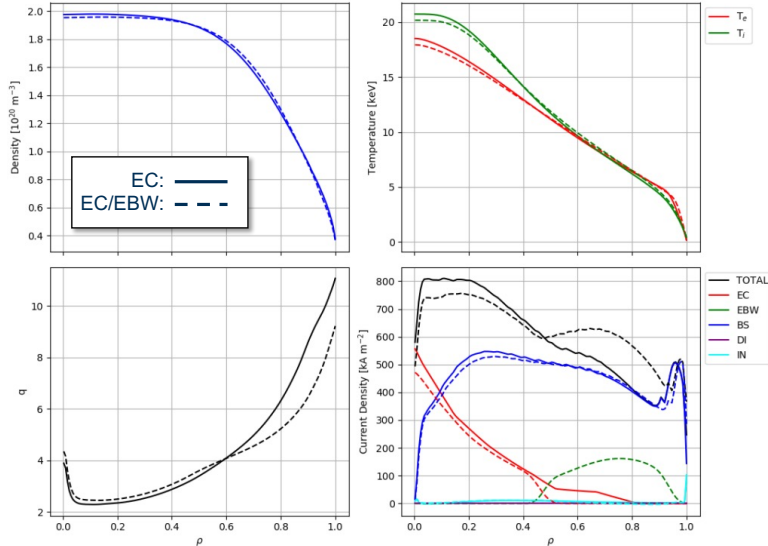

Figure 2: Profiles of the two preferred FTPOs using either pure ECCD (solid) or combined ECCD/EBW heating.

Table 1: Key parameters of the preferred FTOPs.

	FTOP1	FTOP2
HCD technique	EC	EC/EBW
R_{geo} [m]	3.60	
A	1.8	
$B_T (R_{geo})$[T]	3.2	
I_p [MA]	20.9	22.0
κ	2.93	
δ	0.59	0.50
P_{fus} [GW]	1.76	1.77
P_{ECCD} [MW]	150	154
P_{rad} [MW]	338	341
Q	11.8	11.5
β_N	4.4	4.1
f_{BS}	0.88	0.78
$\bar{n}/n_{GW}$ [%]	100	94
l_i (3)	0.26	0.25
η_{CD}^{EC} [A/W]	0.016	0.027
η_{CD}^{EBW} [A/W]	N/A	0.034
P_{sep}/R_{geo} [MW/m]	41	
$(H_{98} + H_{98}^{\star})/2$	1.35	1.19

Preferred FTOP: Assessment of different HCD techniques with respect to grid efficiency, plasma access and tokamak integration strongly favour microwave heating. Two preferred FTOPs with $P_{fus} \approx 1.8\ GW$ have been developed, one with only ECCD and one with ECCD and EBW, after identifying an operational point in B_t and n_e where both ECCD and EBW have access to the plasma. Table 1 gives typical parameters for the two FTOPs and Figure 2 shows the key profiles from f-JETTO. To allow access to ECCD and EBW at $n_e \approx 2 \cdot 10^{20}\ m^{-3}$ $B_t \approx 3\ T$ is required. This is challenging in an ST with $A = 1.8$ and $R_{in} = 1.6\ m$. ECCD is a proven technique but due to the low current drive efficiency $\eta_{CD} \sim 0.016\ A/W$ at high density, a higher H-factor is required to achieve the target $\beta_N = 4.4$. First and 2nd harmonic O-mode in the range of $100 - 240$ GHz cover the entire plasma radius. EBW on the other hand has 3 times higher normalised current drive efficiency ζ_{CD} but due to the high core T_e can only access $\rho > 0.4$. The increased current drive efficiency achieves $P_{fus} = 1.8\ GW$ at lower β_N and lower H_{98} with similar P_{aux}. As the physics base is less mature, and the coupling scheme is more complicated a 1.8 MW EBW system is currently being implemented on MAST-U (operation expected in 2024) to study the physics in an ST. Optimisation is ongoing to extend the radial coverage of the EBW. Central ECCD is always needed as this region is never accessible for EBW due to the Doppler shift of the resonance. The ECCD and EBW current drive efficiencies used in f-JETTO have been iterated with GRAY ray tracing and ray tracing/full-wave GENRAY/CQL3D calculations, respectively. Both

points operate at $f_{GW} \sim 1$ but the peaked density profile caused by the relatively deep pellet deposition to $\rho \approx 0.7$ means that the edge density is likely to be below the Greenwald limit. The discrete pellet model in JINTRAC has been used to optimise the launch geometry and pellet parameters within engineering constraints whilst keeping the edge density perturbation below 5%. Deepest penetration has been found with off-midplane high field side (HFS launch, which has been used for the continuous pellet model in f-JETTO. As expected, the EC/EBW heated scenario requires a less ambitious confinement assumption. The actual value of H_{98} should be taken as indicative only as the turbulence in STEP is dominated by electromagnetic modes (EM) rather than electrostatic (see below). ST specific scaling laws [6] suffer from a rather small database but usually show a stronger dependence on B_t and a weaker dependence on I_p. This could be connected to the dependence of micro tearing modes (MTM) on $\nu^\star$. According to these scaling laws H-factors well below 1 would be sufficient to achieve the STEP parameters. Also the Petty 08 scaling law [7] derived from dimensionless scaling experiments which compares well against JET and MAST data gives lower H values than H_{98}. The α-particles provide strong drive for toroidal Alfvén eigenmodes (TAE). TAEs however are even more strongly damped due to the high β and are stable under STEP FTOP conditions. The no-wall β limit for FTOP1 is $\beta_N^{nW} = 3.9$ and should be similar for FTOP2. Hence, both FTOPs are marginally above the no-wall limit. In-vessel saddle coils for active RWM control are needed for their stabilisation; current design shows that the RWM amplitude can be controlled well below the disruptive limit. $m/n = 3/1$ and $5/2$ neoclassical tearing modes (NTM) are found to be stable for STEP conditions, whilst 2/1 and 3/2 modes are excluded by operating at $q_{min} > 2$. This is due to the strongly negative Glasser-Greene-Johnson term of the modified Rutherford equation. So far only the FTOP has been studied, but the choice of ECCD and EBW as HCD systems would enable the design for pre-emptive NTM control.

Reaching the FTOP: Whilst STEP will be equipped with a small solenoid $\Psi \approx 9\,Vs$ enabling plasma initiation and the establishment of a low current target plasma the remaining 80% -90% of the current must be ramped-up and 100% sustained non-inductively. DYON modelling of the break down using a hexapole null shows burn-through with $V_{loop} \sim 6.5\,V$ well within the capabilities of the currently envisaged solenoid. The modelling includes eddy currents from nearby conducting structures and, in iteration with a free boundary equilibrium code, satisfies radial force balance. With $\sim \frac{1}{2}$ the available solenoid swing, plasma currents around 1-2 MA can be reached. The further inductive flux, modelled with f-JETTO, is used to reach an ohmic full bore HFS limited plasma at small current as target for the non-inductive ramp. The key for the non-inductive phase is to avoid a strong central current-hole due to the back EM force. This can be realised by a $\sim 1/2$ h ramp where the current profile is broadened from the centre. This method has been demonstrated in a smaller $R_{geo} = 2.5\,m$, $I_p = 18\,MA$ concept. ECCD is used at low $f_{GW} \sim 0.25$ to optimise $P_{aux} < 250\,MW$ to reach the full plasma current. Finally, a relatively fast $\sim 10s - 100s$ density ramp to the final density of $f_{GW} \approx 1$ is used to reach the FTOP. The high ECCD power leading to a hot electron $T_e \sim 60\,keV$ plasma with $T_i \sim 5\,keV$ may lead to T_i clamping due to the ITG/TEM turbulence characteristics as recently studied [8] on ASDEX Upgrade and W7-X. Modelling access to the FTOP with the Qualikiz neural network transport model, that captures the relevant ITG/TEM turbulence, suggests that T_i clamping may not be a problem in STEP. The studies optimising the ramp-up are still ongoing and the ramp-down has not yet been addressed.

Transport: Linear GK analysis of STEP-like equilibria has shown that the dominant modes are electromagnetic MTM and kinetic ballooning modes (KBM) [9] rather than electrostatic ion temperature gradient or trapped electron modes as in conventional tokamaks. MTMs at low $k_\perp \rho_s < 0.6$ (iMTMs) are very robust whilst KBMs as well as MTMs on the electron scale are stabilised by a small increase of β' and the diamagnetic flow shear. Local nonlinear GK simulation show that the iMTMs cause dominantly electron transport due to magnetic flutter. These calculations so far show no saturation, but are numerically challenging for local codes due to very extended eigenfunctions along the field line. Saturated MTM simulations showing similar modes using MAST parameters suggest the suppression of zonal flow stabilisation due to the high gradient in the Shafranov shift in STEP. Reduced transport models thought to capture the MTM characteristics and tested against NSTX or MAST as well as GK simulations [10] predict similar electron transport in STEP as assumed by the BgB model though differences in the T_i profiles obtained give large differences in the predicted P_{fus}. This gives further confidence that the FTOP conditions may be achievable. STEP parameters are far from present day devices and reduced model predictions must be considered with great caution. E.g. the model by Rafiq. et.al. [10] for STEP parameters does not agree in the linear phase with GK simulations.

Exhaust: STEP like any future magnetic fusion power plant needs to operate in fully detached conditions to handle the heat loads and avoid excessive target erosion. To address the exhaust challenge in the compact configuration alternative magnetic divertor configurations that increae the flux expansion and the connection length will be used on both inner and outer divertor legs. For the outer divertor an extended leg is the most efficient option, whilst the space restrictions at the inner leg favour a configuration approaching an X-divertor. The latter requires two HFS coils with opposing currents which is an integration challenge. FBE optimisation of the "X-divertor" in conjunction with engineering assessments suggest that this should be feasible. In addition, to protect the inner divertor a double null configuration has been chosen though the divertors are being designed to withstand single null heat loads. The expected narrow scrape-off-layer (SOL) decay length $\lambda_{SOL} < 2\,mm$ means that highly accurate ($\Delta Z < 4\,mm$) absolute and relative vertical position control is needed which is challenging at $\kappa \sim 2.9$. First assessments show that such a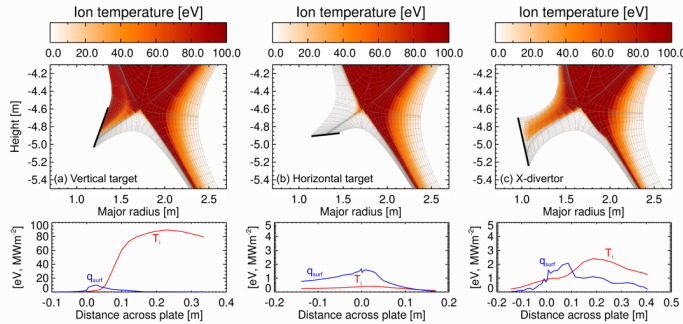ccurate control should be possible using passive stabilisation loops close to the plasma and ITER-like in-vessel coils behind the blankets.

Figure 3: SOLPS-ITER simulations for different target geometries and divertor configurations ($P_{sep}/R \approx 40\,MW/m$, $R_{geo} = 2.5\,m$, $B_t = 2.3\,T$, $I_p = 17.6\,MA$).

The conditions to access strong detachment for both divertor legs using D_2 and Ar injection at different power levels P_{sep} have been studied using SOLPS-ITER with kinetic neutrals but no drifts. mostly using a more challenging smaller design. The validity of the results have been checked in a larger concept that is equivalent to the preferred concept from the exhaust point of view. Figure 3 shows the comparison of a standard vertical target (left) to a horizontal target (middle) and the vertical target "X-divertor" for similar levels of D_2 and Ar injection. Keeping the Ar concentration c_{Ar}, at the separatrix below 1%, acceptable heat loads with $q_{surf} < 10\,MW/m^2$ can be reached in all configurations. With the vertical target only partial detachment can be achieved at acceptable Ar levels. Hot-ions $T_i \approx 90\,eV$ in the far-SOL lead to unacceptable erosion. Both the horizontal target as well as the "X-divertor" reach strong detachment. The integration challenge currently favours the "X-divertor" as the horizontal target configuration will be more difficult to pump and requires a coil close to the X-point, that is difficult to shield. Conditions to reach detachment in the outer leg are of less concern requiring lower Ar levels despite the higher power. The impact of disconnected configurations has also been studied as well as the stability of the detachment front for varying P_{sep}. The database of SOLPS-ITER runs has been used to benchmark a simple model for the detachment operation point represented by a function of neutral pressure p_0 and c_{Ar} with the magnetic configuration also taken into account. This model will be used in the further FBE optimisation as well as the integrated modelling to ensure acceptable exhaust conditions.

Conclusion: Designing an electricity-producing prototype compact fusion power plant has many technical and plasma physical challenges. Over the last 2 ½ years modelling, with newly developed and optimised tools, has greatly increased the confidence in a feasible plasma solution. This has been done in close collaboration with the engineering team to derive a first concept design in the near future. Obtaining a first principle understanding of the plasma transport and the requirement of an H-mode like edge without ELMs remain substantial challenges that still need to be resolved. The latter challenge though is equally difficult for conventional aspect ratio devices such as DEMO. The STEP design however allows a relatively straightforward integration of ELM coils with either the in-vessel RWM coils or the ex-vessel error field correction coils to mitigate this risk.

[1]   STEP - Spherical Tokamak for Energy Production, https://step.ukaea.uk/.
[2]   H. Wilson et.al., in *Commercialising Fusion Energy* (IOP Publishing, 2020), pp. 8.
[3]   J. E. Menard *et al.*, Nuclear Fusion **56**, 106023 (2016).
[4]   Iter Team, Nucl. Fusion **39**, 2137 (1999).
[5]   J. E. Menard, Philosophical Transactions of the Royal Society A: Mathematical, Physical and Engineering Sciences **377**, 20170440 (2019).
[6]   G. S. Kurskiev *et al.*, Nuclear Fusion **62**, 016011 (2021).
[7]   C. C. Petty, Physics of Plasmas **15**, 80501 (2008).
[8]   M. N. A. Beurskens *et al.*, Nuclear Fusion **62**, 016015 (2021).
[9]   B. S. Patel, D. Dickinson, C. M. Roach, and H. R. Wilson, Nuclear Fusion **62**, 016009 (2021).
[10]   T. Rafiq, S. Kaye, W. Guttenfelder, J. Weiland, E. Schuster, J. Anderson, and L. Luo, Physics of Plasmas **28**, 022504 (2021).